A FCM-based image de-noising with spatial statistics pilot study

Tzong-Jer Chen (s838502@oz.nthu.edu.tw)
Wuyi University

Research Article

Keywords: FCM, Residule image, Moran statistics, image de-noise

Posted Date: October 5th, 2022

DOI: https://doi.org/10.21203/rs.3.rs-1802029/v2

A FCM-based image de-noising with spatial statistics pilot study

Tzong-Jer Chen*

Department of Mathematics & Computer Science, Wuyi University, Wuyishan, Fujian, 354300 China.

*Corresponding author:

Tzong-Jer Chen, Ph.D.,

Associate Professor

Department of Mathematics & Computer Science, Wuyi University, Wuyishan, Fujian, 354300 China.

Phone: +86-1809-4158256

E-mail: s838502@oz.nthu.edu.tw

Abstract
Image de-noising is an important scheme to make the image visually prominent and obtain enough useful information. To obtain reliable results, many applications had developed for effective noise suppression and received good image quality. This report assumed a residual image consisted of noises with edges produced by subtracting the original and a low-pass filter smoothed image. The Moran statistics was then using to measure the variation of spatial information in residual images and then as a feature data input to FCM. Three clusters pre-assumed for FCM in this work: they are heavy, medium and less noisy areas. The rates of each position partially belongs to each cluster were determined by a FCM membership function. Each pixel in noisy image assumed in de-noising processing that which is a linear combination of product of three de-noised images with membership function in the same position. Average filters with different windows and a Gaussian filter priori applied to this noisy image to make three de-noised versions. The results showed that this scheme worked better than the non-adaptive smoothing. This scheme‘s performance is evaluated and compared to the Bilateral filter and NLM using PSNR and SSIM. The developed scheme is a pilot study on this area. Further future studies needed on the optimized number of clusters and smoother versions used in linear combination.

Keyword: FCM, Residule image, Moran statistics, image de-noise.

I. Introduction

The noise is a major source of digital image contamination. Image noise may arise from quantization of the image data, transmission errors, electronic interference from the imaging hardware, as well as from other sources [1]. The noise in digital image affected the real image signal resulted in image quality decline. This influence will affect the performances of digital image application areas such as, segmentation, retrieval, edge extraction etc... To obtain reliable results, efforts had been in many applications for effective noise suppression. Image de-noising, in the field of image procession, is a commonly used method to make the image visually prominent and obtain enough useful information [2, 3].

The major function of image de-noising is to recover the original image from a noisy measurement and retain image structure information as much as possible [4]. The de-noising is a well known, using from time to time, but an ill-posed problem in image processing. To date, schemes of de-noising in digital image developed continuously. From pixel level filtering methods, such as Gaussian filtering, Bilateral filtering and total variation regularization, to patch level filtering methods, such as non-local means [3, 5, 6], block-matching 3D filtering (BM3D) [4], and low-rank regularization and so on [3,7].

Tomasi *et al.* introduced Bilateral filtering as a nonlinear filter that combined domain and range filtering [8]. This filter replaces each pixel with the weighted average of its neighbors. The weight assigned to each neighbor decreases with both the distance in the image plane and the distance on the intensity axis [6]. This filter made a smooth image while preserving the edges. It demonstrated great effectiveness for a variety of computer vision and computer graphics problems [6]. The non-local mean filtering proposed by Buades *et al.* [4] is a spatial image de-noising algorithm based on Bilateral filtering. This de-noising method replaced

each pixel in the noisy image using the weighted pixel average with the related surrounding neighborhoods. The weighting function is determined by the similarity between neighborhoods [9]. It was applied to image de-noising in various specific fields because of its superiority performance over other methods, such as the Means filter and Bilateral filtering [9, 10].

To estimate white Gaussian noise in images, a work surveyed six methods and found that the noise estimation using standard deviation measurement in residual images was most reliable [11]. The residual image obtained by subtracting the original and a low-pass filter smoothed image. Chuang *et al.* measured the noise level directly from the residual image bit plane. They claimed that the noise level estimation in the original image might be overestimated due to the nature of the quantization involved [12]. A residual image (RE) can be defined as RE = OR − SM using the subtraction value between an original (OR) image and its smoothed (SM) version. The subtraction can effectively remove the signal part and leave the noise with edge parts [12, 13].

Many RE based state-of-the-art de-noise algorithms were proposed in past decades. Baloch *et al.* developed a RE correlation regularization de-noising scheme that minimizes the correlation between neighboring RE patches [14]. They claimed that the correlation-based regularization can help produce much better results than the K-SVD (a dictionary learning algorithm), both qualitatively and quantitatively. However, a computational burden drawback exists in the algorithm. Wang *et al.* proposed a residual-based method that combined the bilateral filter and structure adaptive kernel filter for Gaussian noise de-noising [15]. The noise was suppressed efficiently and this combined method showed acceptable de-noising performance for heavy Gaussian noise. However, the iterations are also a time consuming task [1]. This method uses a

novel criterion for determining wavelet coefficient thresholds by minimizing the computed RE image kurtosis. Roychowdhury *et al.* estimated noise in chest CT image data with varying image quality using RE [16].

The RE should possess the statistical properties of contaminating noise. However, it is very likely that the residual patch contains remnants from the clean image patch [14]. As a result, at high noise levels, the RE usually contains structures from the clean image patch; thus, it does not contain contaminating noise. Brunet *et al.* applied a statistical test on the RE and found that RE did not contain only pure noise; as there were structures present [13]. They de-noised RE with an adaptive Wiener filter first and then parts of the cleaned RE where one of the hypothesis tests was rejected were added back into the de-noised image. The idea is to first smooth the image flat regions, and then work on the details. Their iterative scheme produced gains in both PSNR and SSIM.

Adaptive de-noising involved newly proposed algorithms that performed local image computation in contrast to global de-noising [17]. These schemes improved the image quality and edge conservation more effectively than the global methods [18-24]. The adaptive image de-noising filter has become a promising research area [20].

A nonlinear module, named the Moran statistic showed correlation with the noise level of medical images [12]. The Moran's Z measurements presented high consistency with the variation in smoothing and sharpening in images [25]. This calculation proved that spatial correlation corresponds well with the variation in image spatial properties [26, 27]. Both Chen *et al.* and Hung *et al.* recently proposed using Moran statistics calculation as index for image de-noising [25-28]. In their work the Moran statistics based adaptive image filter algorithms produced better image quality than global methods.

Fuzzy c-means (FCM) clustering is an unsupervised scheme successfully applied to feature analysis, clustering, and classifier designs [29, 30]. The FCM algorithm classifies the image by grouping similar data points in the feature space into clusters, if the images are presented in “feature spaces”. The FCM algorithm assigns pixels to each category by using fuzzy memberships. Each point in feature space is partially belonging to the clusters by fuzzy membership function.

This work proposed estimation the spatial information of smoothness and sharpness in RE images by Moran statistics. The measurements of Moran’s Z was then using as feature data input to FCM. Three clusters pre-assumed for FCM in this work: they are heavy noisy, medium noisy and less noisy areas (i.e. structure areas). The rates of each position partially belongs to clusters were determined by a FCM membership function. The membership function uses as a weight to calculate the weighted sum of each position. Each pixel in a noisy image is a linear combination of the product of three SMs with membership functions in the same position. The average filters with different window (3×3, 5×5) and a Gaussian filter priori applied to this noisy image to make three SMs. The results showed that this scheme worked better than the non-adaptive.

The performance of this scheme is evaluated in terms of the peak signal-to-noise ratio (PSNR), structural similarity index (SSIM) and comparison to the bilateral filter and NLM.

2. Methods and Materials

2.1RE

The smoothed image is obtained by averaging the neighboring pixels in a mask, i.e., using a 3×3 or 5×5 average filter. The RE_3can be defined as $RE_3 = OR – SM_3$using the subtraction value between an original (OR)

image and its smoothed version (SM_3). The SM_3 is produced using a 3×3 window and SM_5 using a 5×5 window, respectively.

2.2 Moran test

The spatial autocorrelation was clarified as follows: "Spatial autocorrelation refers to the fact that the value of a variable at one point in space is related to the value of that same variable in a nearby location." [28, 31]. The spatial information concept has long been used in image de-noise and image quality estimation with different format types [25-28]. To determine the spatial autocorrelation, Moran introduced *AC* to measure the degree of spatial autocorrelation in area data [31, 32]. *AC* shows in the following equation, and its range is between −1 and 1:

$$AC = \frac{N \sum_{j=1}^{r\times c} \sum_{i=1}^{r\times c} \delta_{ij}(x_i-\bar{x})(x_j-\bar{x})}{S_0 \sum_{i=1}^{r\times c}(x_i-\bar{x})^2} \quad (1)$$

Where x_i is the gray level for pixel i, $\bar{x}$ is the mean window gray level, $S_0 = 2(2mn - m - n)$, m and n are the number of rows and columns in the window, N is the total number of pixels in the window, and $\delta_{ij} = 1$ if pixel i and j are adjacent and 0 otherwise. A larger *AC* value means greater correlation between the pixels and that the area is not likely a noise. When the size of N is large enough (>25), the variable *AC* approximately follows a normal distribution with the mean and variance given by

$$a = -1/(N-1) \quad (2)$$

and

$$\sigma^2 = \frac{N[(N^2-3N+3)S_1 - NS_2 + 3S_0^2] - K[N(N-1)S_1 - 2NS_2 + 6S_0^2]}{(N-1)(N-2)(N-3)S_0^2} - a^2 \quad (3)$$

where $K = N\sum(x_i-\bar{x})^4 / [\sum(x_i-\bar{x})^2]^2$, $S_1 = 2S_0$, and $S_2 = 8(8mn - 7m - 7n + 4)$. We can use the standardized normal statistic

$$Z = \frac{AC-a}{\sigma} \quad (4)$$

to determine the feature of an image.

A higher Z will lead to null hypothesis rejection making the image noisy. This means that more structured information exists in this area and random noise is less likely in the image [12]. Based on this premise, the Moran *Z* value has successfully been applied to present the image spatial features [18, 19, 25-27, 33]. The Moran statistics used in this work divide the noisy areas in the RE.

2.3Fuzzy c-means (FCM)

Fuzzy c-means (FCM) clustering is an unsupervised technique successfully applied to feature analysis, clustering, and image segmentation [29]. The FCM algorithm classifies the image by grouping similar data points in the feature space into clusters if that image is represented in various feature spaces. Every pixel is assigned to each category partially using fuzzy memberships. Let $\boldsymbol{X=(x_1, x_2,\ldots, x_N)}$ denotes a feature space with $\boldsymbol{N}$ points to be partitioned into $\boldsymbol{M}$ clusters, where $\boldsymbol{x_j}$ represents multispectral (features) data point. The algorithm is an iterative optimization that minimizes the cost function defined as follows:

$$J = \sum_{j=1}^{N}\sum_{i=1}^{M} u_{ij}^{m} \, \mathrm{P}x_j - c_i \, \mathrm{P}^2 \quad (5)$$

where $\boldsymbol{u_{ij}}$ ($\in [0,1]$)indicating the degree that the sample $\boldsymbol{x_j}$ belongs to the cluster center $\boldsymbol{c_i}$ and $\sum_{i=1}^{M} u_{ij} = 1$, The fuzziness of the resulting partition increases with *m*. In this study, *m*= 2 was used, $\boldsymbol{c_i}$ is the ith cluster center it can be calculated as:

$$c_i = \frac{\sum_{j=1}^{N} u_{ij}^m x_j}{\sum_{j=1}^{N} u_{ij}^m} \quad (6)$$

$$u_{ij} = \frac{1}{\sum_{k=1}^{M} \left(\frac{\mathrm{P}x_j - c_i \mathrm{P}}{\mathrm{P}x_j - c_k \mathrm{P}} \right)^{\frac{2}{m-1}}} \quad (7)$$

Starting with an initial guess for each cluster center, the FCM will converge to a solution for c_i representing the local cost function minimum. The iteration is stopped when the maximum difference between two cluster centers at two successive iterations is less than a threshold (=0.00001). The FCM implemented by using the Matlab, version 2017b (9.3.0.713579).

3. Experiments and Results

The RE consists of both noises and edges. It means that each pixel in RE contained partially noises and edges. The RE shows more edges than noises if decreasing the passing degree when applied a low pass filter in image and vice versa. The more blurred SM image can be get when increase the window size of an average filter or decreasing passing rate. In the same way, this processing produced more of noises and edges in a RE too.

3.1 Experiments

A noisy Barbara as showed in Figure 1 was used to demonstrate the above assumption. Gaussian white noise was padded to this image first (μ=100, σ= 10, on 20% of the entire image padded randomly) and then filtered with a 3×3 and a 5×5 average filter to generate RE_3 and RE_5,

respectively. Following this, measured Moran's Z in both RE.

The Moran's Z presented that spatial correlation which corresponds well with the variation in image spatial properties. A higher Z value means less noise and more structures in an area and vice versa. The spatial properties showed using Moran's Z histogram for RE_3 and RE_5 are different apparently, as shown in Figure 2.The Moran's Z were measured using a 5×5 sliding window. It is obviously that the curve of RE_5 shift to high Z area than RE_3 gets. The result shows that there are more structure areas in RE_5 than in RE_3. The spatial autocorrelation scheme clarified spatial information in images.

This Moran's Z measurements were then used as feature data in FCM algorithm. Three clusters are pre-assumed for FCM in this work: they are heavy noisy (lowest Z area), medium noisy and less noisy areas (highest Z area), as showed in Figure 3. This figure shows also three center points of cluster in the feature domain, where Moran's Z values of RE_3 and RE_5 are coordinates. Each point in feature data space own three membership rates.

3.2 Results

The proposed scheme assumed that the filtering process is a linear combination of product of three SMs with membership function. The average filters with two different window (3×3, 5×5) and a Gaussian filter (σ=0.5) priori applied to this noisy image to make three SMs. In this work, SM_5 was used for heavy noisy, SM_3 for medium and $SM_{0.5}$ for less noisy or edge areas.

Six frequently used images were selected in this work, as shown in Figure 4. These test images, all size 512×512 and 9 bits deep. Then various Gaussian noise were priori-added to these images and can be divided as three groups as: 1. padded randomly on 20%, 50%, 75% of the

entire image with μ=0 and σ= 20, 30, 50, 60; 2. padded randomly on 50% of the entire image with μ=30 and σ= 20, 30, 50, 60; 3. padded randomly on 20% of the entire image with μ=100 and σ= 10, 15, 20, 30, respectively.

The average filter with window (3×3, 5×5), a Gaussian filter (σ=0.5), Bilateral filter [34], Non-local mean scheme [35] and proposed algorithm were applied to these noisy images. The PSNR and SSIM [36] were calculated and show in Figures 5-10.

Figures 5-7show PSNR results, Figures 8-10 show results of SSIM on de-noised images, in these figures (a): added 20%, μ=0 with various σ , (b): added 50%, μ=0 with various σ, (c): added 75%, μ=0 with various σ, (d): added 50%, μ=30 with various σ, (e): added 20%, μ=100 with various σ.

The image qualities depend on PSNR and SSIM values. For both indices, the high the values correspond to the better quality. The high the $\boldsymbol{\sigma}$ can make the noise variations in image. This variation can decline the quality of images. The abscissas in Figure 5-10 show variations of σ. Both indices of PSNR and SSIM show descent to respond ascent variation of $\boldsymbol{\sigma}$.

Some proposed scheme results, a linear combination of SM_5, SM_3 and $SM_{0.5}$, are superior to the single de-noise filter. We can see that in Figure 7-10. Most proposed scheme results are better than the Bilateral filter and some even better than NLM. The quality indices results from this novel scheme are not always superior to the single filter but most are good.

4. Discussions

4.1 Noisy levels with membership function

In this work, the scheme assumed that the filtering process is a linear combination of product of three SMs with membership function. The lower Z areas assigned to heavy noisy, middle areas assigned to medium noisy and higher Z areas assigned to edge or less noisy. Each pixel in noisy image assumed partially belonging to three partitions and has membership partition rates in the same position. The SM_5 used for heavy noisy and make product with the rate of left areas. The SM_3 and $SM_{0.5}$ used for medium, less noisy or edge and make product with the rate of areas. These areas show in Figure 3.

To prove above assumption is correct, if changed the SMs correspond to original assigned noisy areas (i.e. arbitrary exchange SM_5, SM_3, $SM_{0.5}$ to any areas), and make product with the rates of those areas. To test, a noisy Barbara (μ=100, σ= 10, 20% randomly added) filtered with a 3×3 and a 5×5 average filter and a Gaussian filter (σ=0.5) applied to this noisy image to make three SMs, respectively. The results of both PSNR and SSIM for all exchange cases are obvious worse than those have done before. This effect shows consistent with previous report of the Moran statistics [32].

However, if assigned the SM_5 to heavy noisy areas and SM_3, $SM_{0.5}$ make product with the rate of left areas or middle areas or exchange even using same SM in two areas. The PSNR and SSIM results for all cases are just a little lower or equal than those performed before. This indicates that proper SM_s selection is important.

4.2 Number of Clusters

Three clusters pre-assumed for FCM in this plot study. There are heavy, medium and less noisy or edge areas, as showed in Figure 3. A lower number of clusters should make the de-noise image approach results similar to a single filter. A higher the number of clusters will get

better results. However, ensuring proper de-noised scheme selection and applying them correctly is a difficult issue.

5. Conclusions

This work proposed estimation the variation of spatial information in RE images by Moran statistics. The Moran's Z measurements were used as feature data in FCM. Three clusters were pre-assumed for FCM in this work: they are heavy, medium and less noisy or edge areas. The rates of each position partially belongs to clusters were determined by a FCM membership function. The membership function uses as a weight to calculate the weighted sum of each position. Each pixel in noisy image assumed that which is a linear combination of product of three SMs with membership function in the same position.

The average filters with two different window (3×3, 5×5) and a Gaussian filter (σ=0.5) priori applied to this noisy image to make three SMs. Six frequently used images were choice in this work. To test, various Gaussian noises were priori-added to these images and then de-noised using proposed scheme.

The performance of this scheme was evaluated in terms of the PSNR, SSIM and made comparison to the Bilateral filter and NLM. Some results from the proposed scheme are superior to the single de-noise filter and most are better than the bilateral filter and some better than NLM. The quality indices results from the novel scheme is not always superior to the single filter but most are good.

The scheme is a pilot study on image de-noising. In the future, further researches on the optimized number of clusters and better smoothed or structure versions using in linear combination are needed to optimize this scheme.

6. Declarations

Ethics approval and consent to participate:

Not applicable

Consent for publication:

Not applicable

Availability of data and materials:

Not applicable

Competing interests:

The author declared that I have no competing interests.

Funding:

Not applicable

Authors' contributions:

Tzong-Jer Chen done all.

Acknowledgments:

I would like to thank Prof. KS Chuang of the National Tsing-Hua University for his help in editing and advising on this article.

Authors' information (optional):

Tzong-Jer Chen*, Department of Mathematics & Computer Science, Wuyi University, Wuyishan, Fujian, 354300 China.

*Corresponding author: Tzong-Jer Chen, Ph.D., Associate Professor

Phone: +86-1809-4158256

E-mail: s838502@oz.nthu.edu.tw

References

1. Hearn TA and Reichel L. Image denoising via residual kurtosis minimization. *Numerical Mathematics: Theory, Methods and Applications*.2015;8, 406–424.

2. Xiao X, Lai J. Image Denoising by Zernike-Moment-Similarity Collaborative Filtering. *Journal of Image and Signal Processing JISP*. 2013; 2, 1-7.

3.Yue H, Sun X, Yang J, Wu F. Image Denoising by Exploring External and Internal Correlations. *IEEE Transactions on Image Processing*. 2015; 24 , 1967-1981.

4. Buades A, CollB, Morel JM.A non-local algorithm for image denoising. *Proceedings of IEEE Conference on Computer Vision and Pattern Recognition, Washington*, 2005; 60-65.

5. Chaudhury KN. Acceleration of the shiftable o(1) algorithm for bilateral filtering and nonlocal means. *IEEE Transactions on Image Processing* 2013; 22(4), 1291-1300.

6.Paris S, Durand F. A Fast Approximation of the Bilateral Filter Using a Signal Processing Approach. In: *Leonardis A., Bischof H., Pinz A. (eds) Computer Vision – ECCV 2006. ECCV 2006. Lecture Notes in Computer Science*, vol 3954. Springer, Berlin, Heidelberg.

7. Dong W, Shi G, Li X. Nonlocal image restoration with bilateral variance estimation: A low-rank approach. *IEEE Trans. Image Process.* 2013; 22, 700–711.

8. Tomasi C, Manduchi R. Bilateral filtering for gray and color images. In: *Proc. of International Conference on Computer Vision, IEEE* 1998; 839–846.

9.Huang L. Improved Non-Local Means Algorithm for Image Denoising, *Journal of Computer and Communications* 2015; 3, 23-29.

10.Zhan Y, Ding M, Xiao F and Zhang X. An Improved Non-local

Means Filter for Image Denoising. I*nternational Conference on Intelligent Computation and Bio-Medical Instrumentation* 2011;14-17, Wuhan, Hubei, China.

11. Olsen SI. Estimation of Noise in Images: An Evaluation. *CVGIP: Graphical Models And Image Processing*1993; 55(44), 319-323.

12. Chuang KS and Huang HK. Assessment of noise in a digital image using the join-count statistic and Moran test. *Phys. Med. Biol.* 1992; 37, 357-369.

13. Brunet D, Vrscay ER, Wang Z. The Use of Residuals in Image Denoising. *in Image Analysis and Recognition, M. Kamel and A. Campilho, Eds., vol. 5627 of Lecture Notes in Computer ScienceICIAR09* 2009; 1–12, Springer.

14. Baloch G, Ozkaramanli H, Yu R. Residual Correlation Regularization Based Image Denoising, *IEEE Signal Processing Letters*2018; 25(2): 298-302.

15. Wang J, Chen Y, Li T, Lu J, Shen L. A Residual-Based Kernel Regression Method for Image Denoising. *Mathematical Problems in Engineering* 2016; Article ID 5245948, 13 pages.

16.Roychowdhury S, Hollcraft N, Alessio AM. Blind analysis of CT image noise using residual denoised images. *IEEE Nuclear Science Symposium and Medical Imaging Conference* (NSS/MIC) 31 Oct.-7 Nov. 2015 San Diego, CA, USA

17.Guo F, Zhang C, Zhang M. Edge-preserving image denoising. *IET Image Process.* 2018; 12 (8), 1394-1401.

18. Chen TJ *et al.*, A novel edge-preserving filter for medical image enhancement. *Computer Graphics, Visualization, Computer Vision and Image Processing* 2017, Lisbon, Portugal, 279-384.

19. Chen TJ. Moran's Z based adaptive image filter. *Computer Graphics, Visualization, Computer Vision and Image Processing* 2018, Madrid

Spain, 382-386.
20. Lu RH and Chen TJ. Adaptive Image De-noising Method Based on Spatial Autocorrelation. *ISICDM* 2018, Chengdu, China; 125-128.
21. Xu, G, and Tan J. Adaptive efficient non-local image filtering. *Journal of Image & Graphics*2012; 17 (4) :471-479.
22. Elfallah AI, and Ford GE. Nonlinear adaptive image filtering based on inhomogeneous diffusion and differential geometry. *Proceedings of SPIE - The International Society for Optical Engineering* 1994; 2182, 49-63.
23. Stawiaski J, and Meyer F. Minimum spanning tree adaptive image filtering. *IEEE International Conference on Image Processing* 2010; 2221-2224.
24. Lin LH and Chen TJ. A novel scheme for image sharpness using inflection points. *International Journal of Imaging Systems and Technology* 2020; 30:753–760.
25. Chen TJ, Chuang KS, Wu J, Chen SC, Hwang IM and Jan ML. A novel image quality index using Moran I statistics. *Phys Med Biol* 2003; 48: N131-N137.
26. Chen TJ, Chuang KS, Wu J, Chen SC, Hwang IM, Jan ML. Quality Degradation in Lossy Wavelet Image compression. *J Digital Imaging* 2003; 16: 210-215.
27. Chen TJ, Chuang KS, Chiang YC, Chang JH, Liu RS.A statistical method for evaluation quality of medical images: Case study in bit discarding and image compression. *Comput. Med. Imaging Graph.* 2004; 28:167-175.
28. Hung CC and Chang ES. Moran's I for impulse noise detection and removal in color images. *J Electronic Imaging* 2017; 26(2), 309-318.
29. Chuang KS, Tzeng HL, Chen S, Wu J, Chen TJ. Fuzzy c-means clustering with spatial information for image segmentation. *Computerized Medical Imaging and Graphics* 2006; 30, 9–15.

30. Lyer NS, Kandel A, Schneider M. Feature-based fuzzy classification for interpretation of mammograms. *Fuzzy Sets Syst* 2002; 114:271–80.

31.Cliff AD and Ord JK. 1981. Spatial process: models and applications. Pion, London, UK.

32. Moran P. The interpretation of statistical maps. *J. R. Stat. Soc. Ser.*1948; B10, 243–251.

33. Lin LH, Chen TJ. Image quality assessment by an efficient correlation-based metric. *Concurrency Computat PractExper.* 2020; e5794. https://doi.org/10.1002/cpe.5794.

34. http://people.csail.mit.edu/jiawen/

35. Goossens B, Luong HQ, Pizurica A, Philips W. An improved non-local means algorithm for image denoising. *in International Workshop on Local and Non-Local Approximation in Image Processing*2008 (LNLA2008),Lausanne, Switzerland, Aug. 25-29.

36.Wang Z, Bovik AC, Sheikh HR, Simoncelli EP. Image quality assessment: From error visibility to structural similarity. *IEEE Trans. Image Process.*2004; 13(4), 600–612.

List of Figures

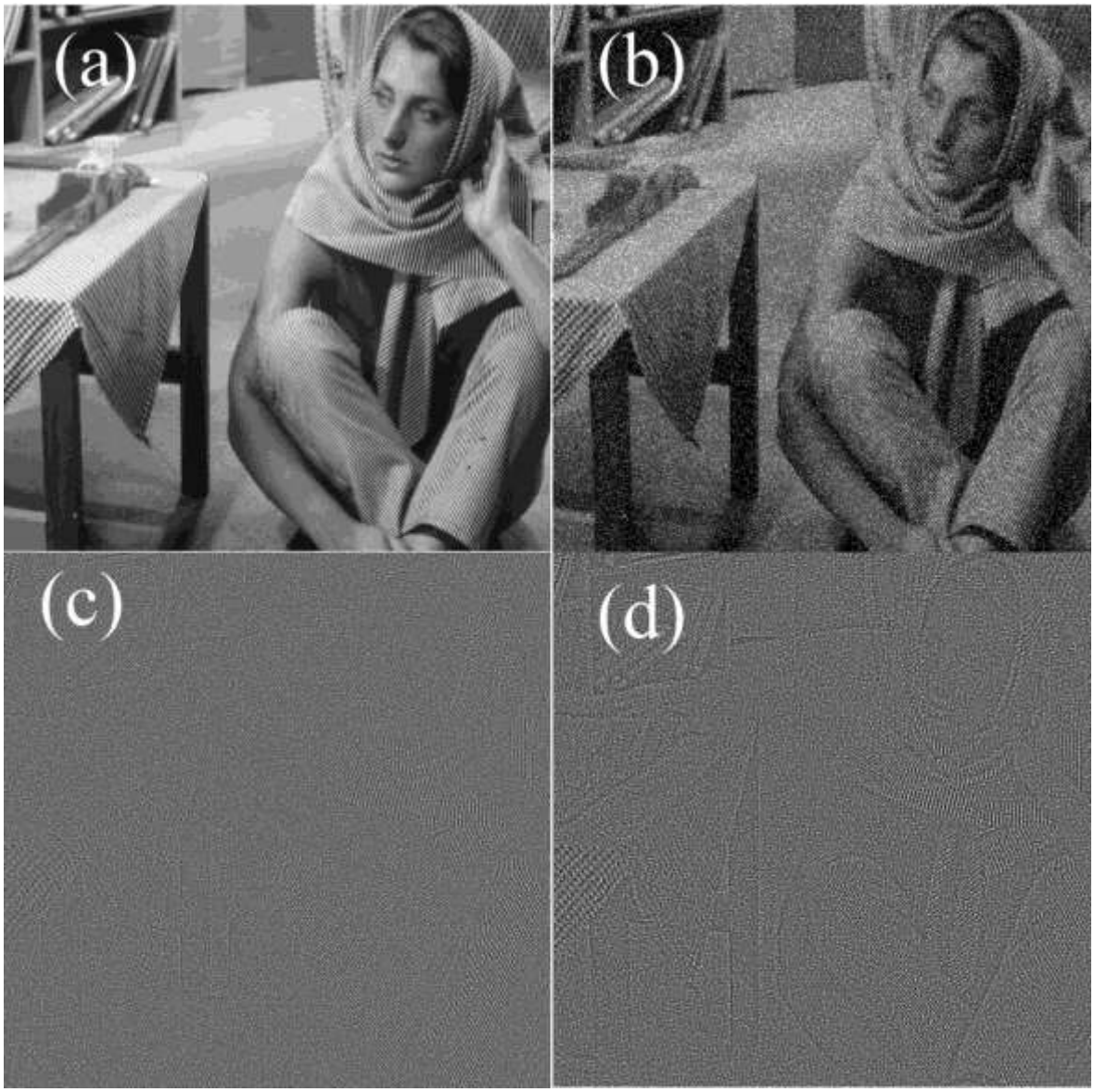

Figure 1. (a) original Barbara, (b)Noisy image, (c)RE_3. (d)RE_5

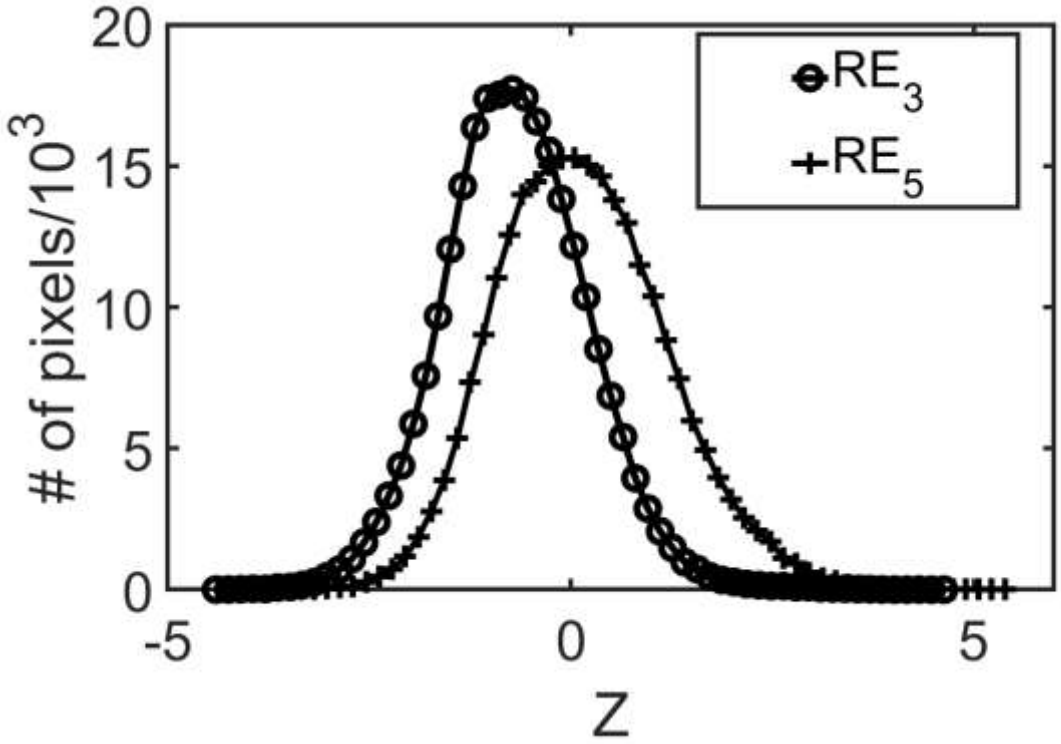

Figure 2. The histogram of Moran Z for RE_3 and RE_5 of noisy Barbara.

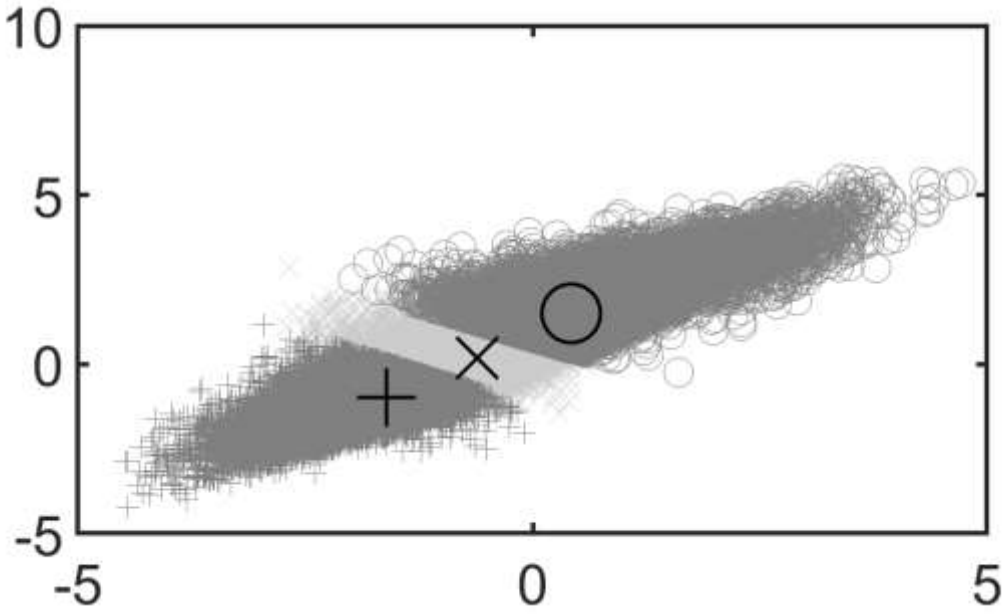

Figure 3. The calculated centroids of cluster in the feature domain (where Moran's Z values of RE_3 and RE_5 are coordinates). ○= less noisy or edge, X= medium noisy, += heavy noisy.

Figure 4. Six images were used in this work: (up left to right) Barbara, boat, hill, (down left to right) Lena, man, and Pentagon.

Figure 5. PSNR after de-noise of Barbara (left) and boat (right), (a) added 20%, μ=0 with various σ, (b) added 50%, μ=0 with various σ, (c) added 75%, μ=0 with various σ, (d) added 50%, μ=30 with various σ, (e) added 20%, μ=100 with various σ.

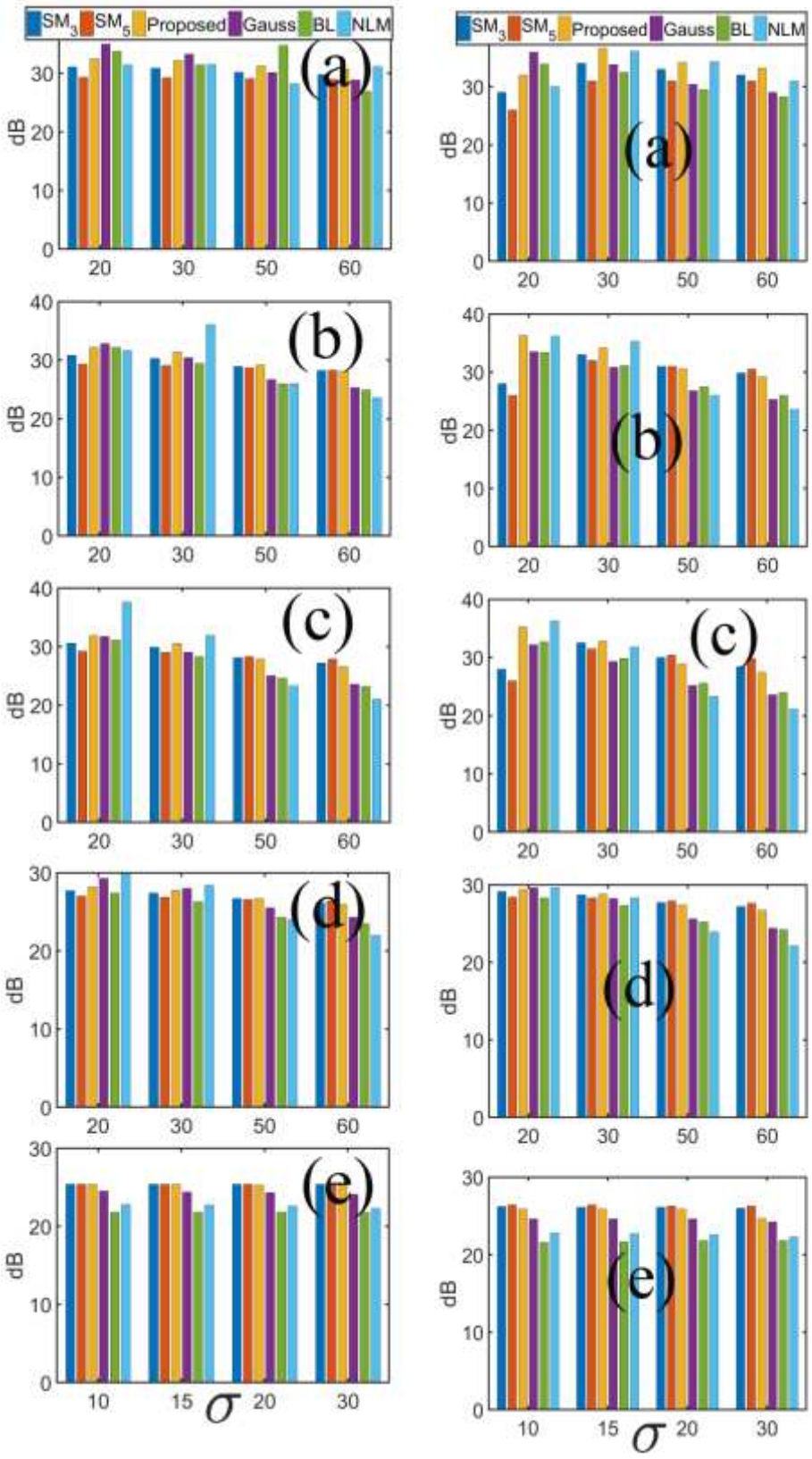
SM3
SM5
Proposed
Gauss
BL
NLM
(a)
(b)
(c)
(d)
(e)
dB
σ
20
30
50
60
10
15

Figure 6. PSNR after de-noise of hill (left) and Lena (right), (a) added 20%, μ=0 with various σ, (b) added 50%, μ=0 with various σ, (c) added 75%, μ=0 with various σ, (d) added 50%, μ=30 with various σ, (e) added 20%, μ=100 with various σ.

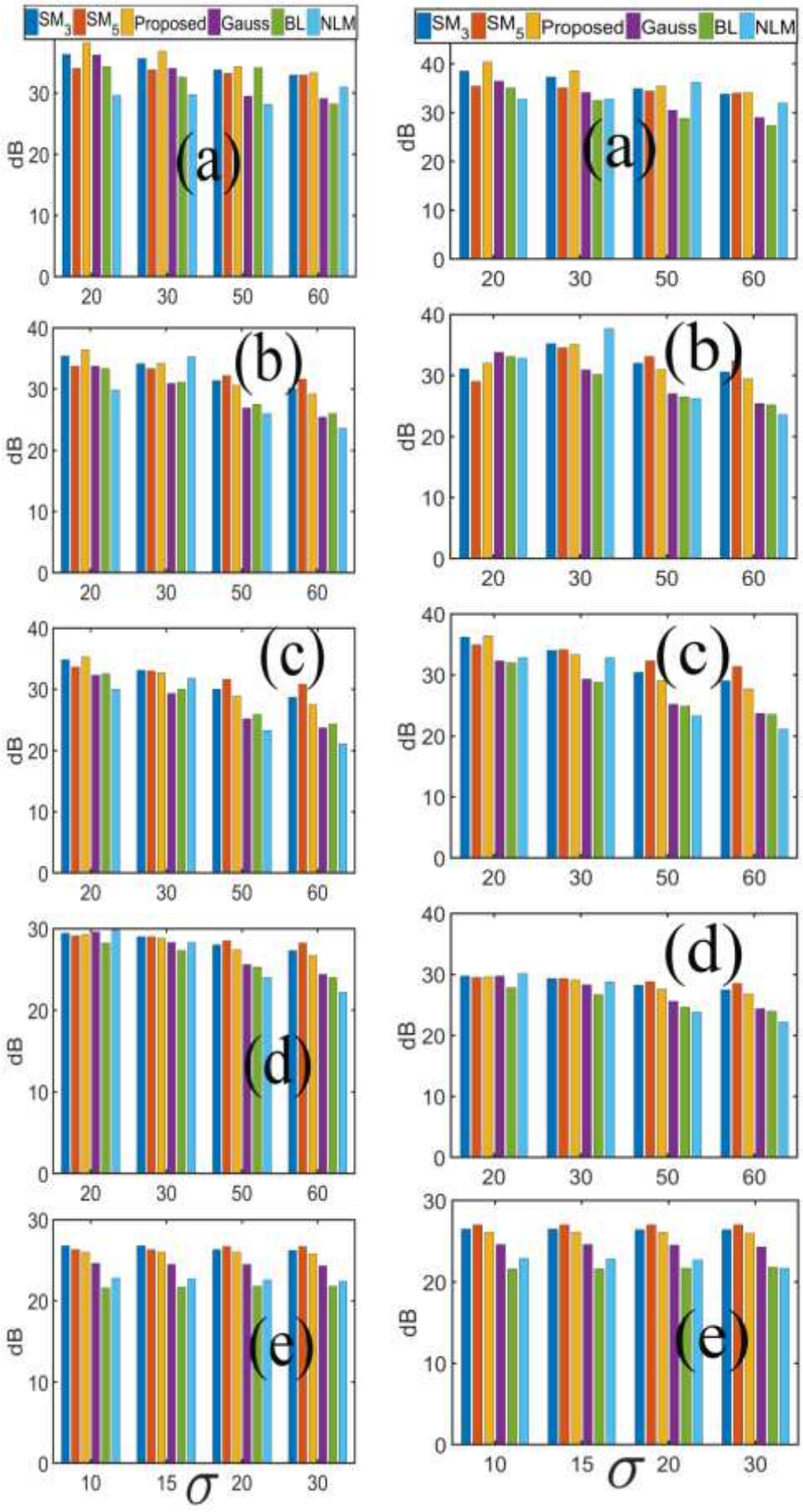
SM3
SM5
Proposed
Gauss
BL
NLM
dB
(a)
(b)
(c)
(d)
(e)
20
30
50
60
10
15
σ

Figure 7. PSNR after de-noise of man (left) and Pentagon (right), (a) added 20%, μ=0 with various σ, (b) added 50%, μ=0 with various σ, (c) added 75%, μ=0 with various σ, (d) added 50%, μ=30 with various σ, (e) added 20%, μ=100 with various σ.

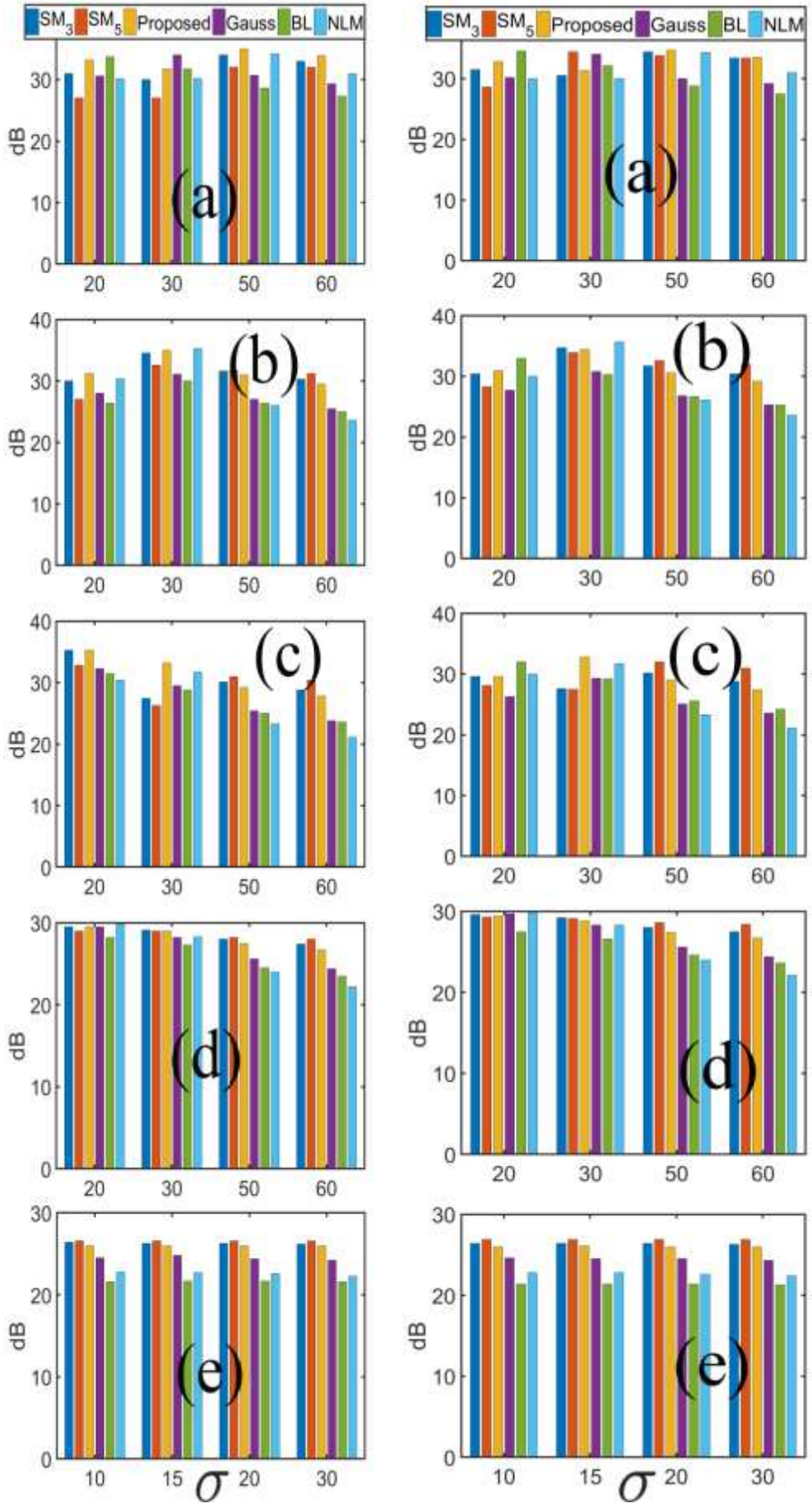
SM3
SM5
Proposed
Gauss
BL
NLM
dB
(a)
(b)
(c)
(d)
(e)
20
30
50
60
10
15
σ

Figure 8. SSIM after de-noise of Barbara (left) and boat (right), (a) added 20%, μ=0 with various σ, (b) added 50%, μ=0 with various σ (c) added 75%, μ=0 with various σ (d) added 50%, μ=30 with various σ (e) added 20%, μ=100 with various σ.

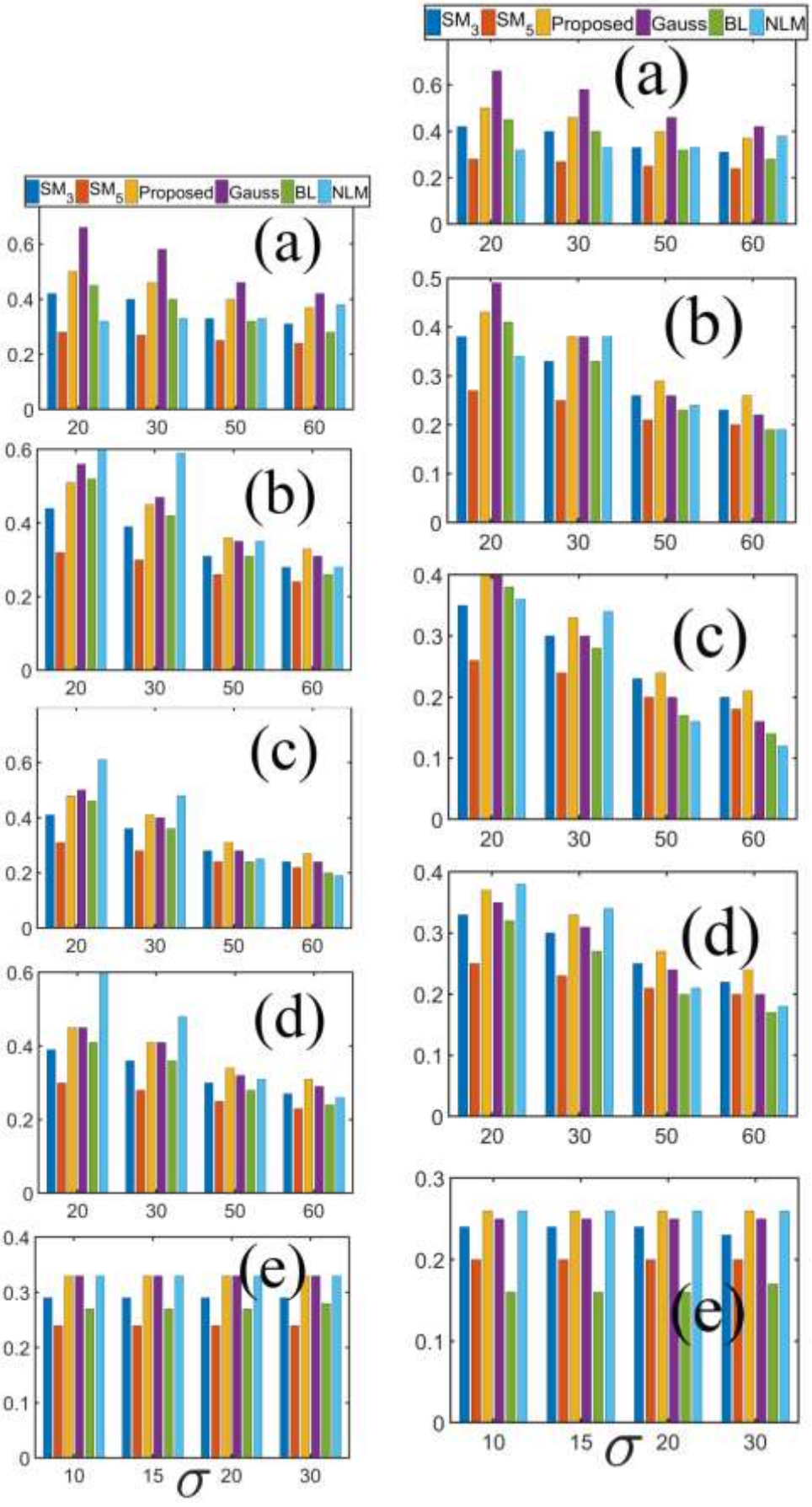
SM3
SM5
Proposed
Gauss
BL
NLM
(a)
(b)
(c)
(d)
(e)
0
0.1
0.2
0.3
0.4
0.5
0.6
10
15
20
30
50
60
σ

Figure 9. SSIM after de-noise of hill (left) and Lena (right), (a) added 20%, μ=0 with various σ,(b) added 50%, μ=0 with various σ (c) added 75%, μ=0 with various σ (d) added 50%, μ=30 with various σ (e) added 20%, μ=100 with various σ.

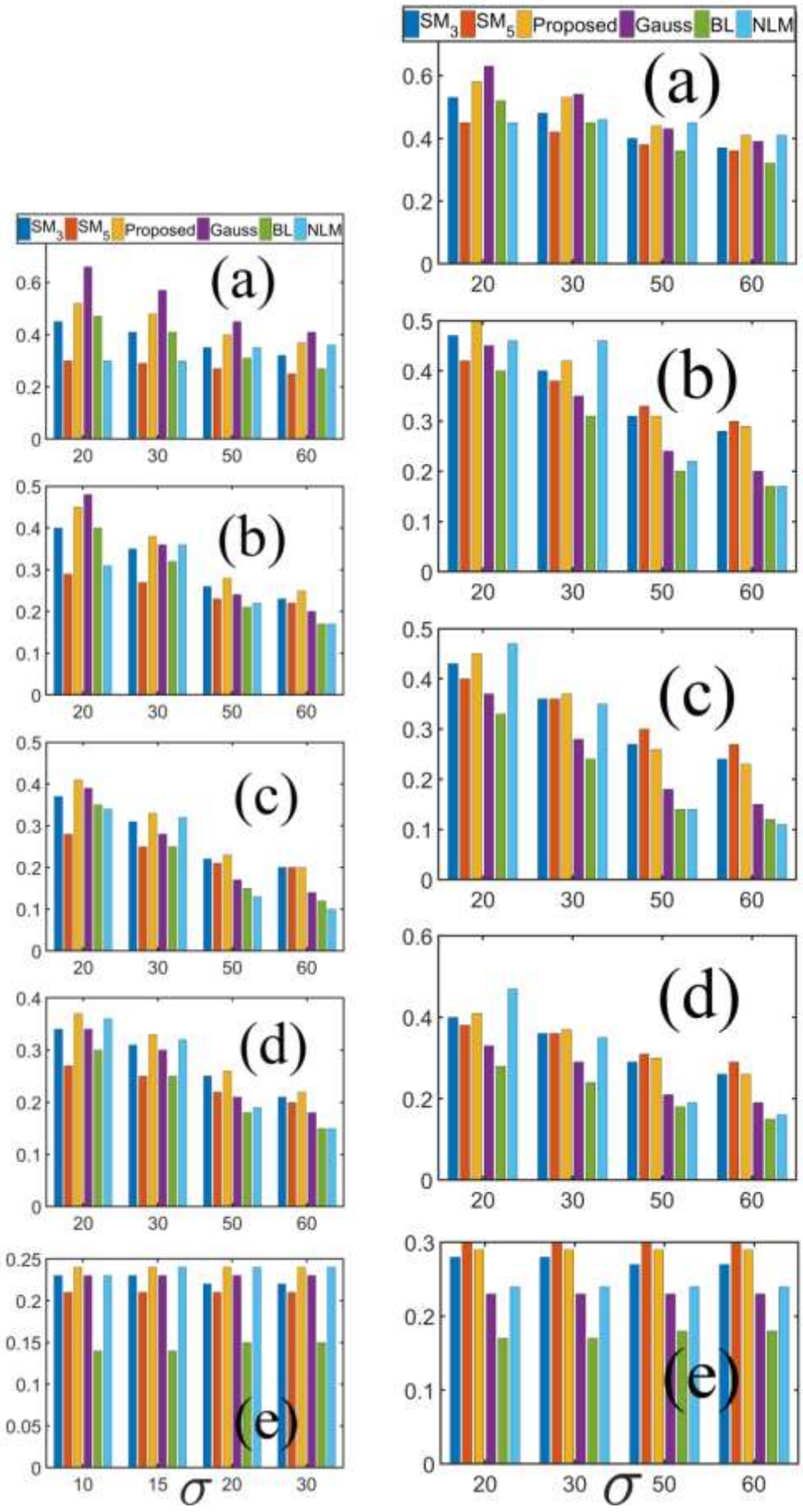
SM3
SM5
Proposed
Gauss
BL
NLM
(a)
(b)
(c)
(d)
(e)
σ

Figure 10. SSIM after de-noise of man (left) and Pentagon (right), (a) added 20%, μ=0 with various σ, (b) added 50%, μ=0 with various σ (c) added 75%, μ=0 with various σ (d) added 50%, μ=30 with various σ (e) added 20%, μ=100 with various σ.

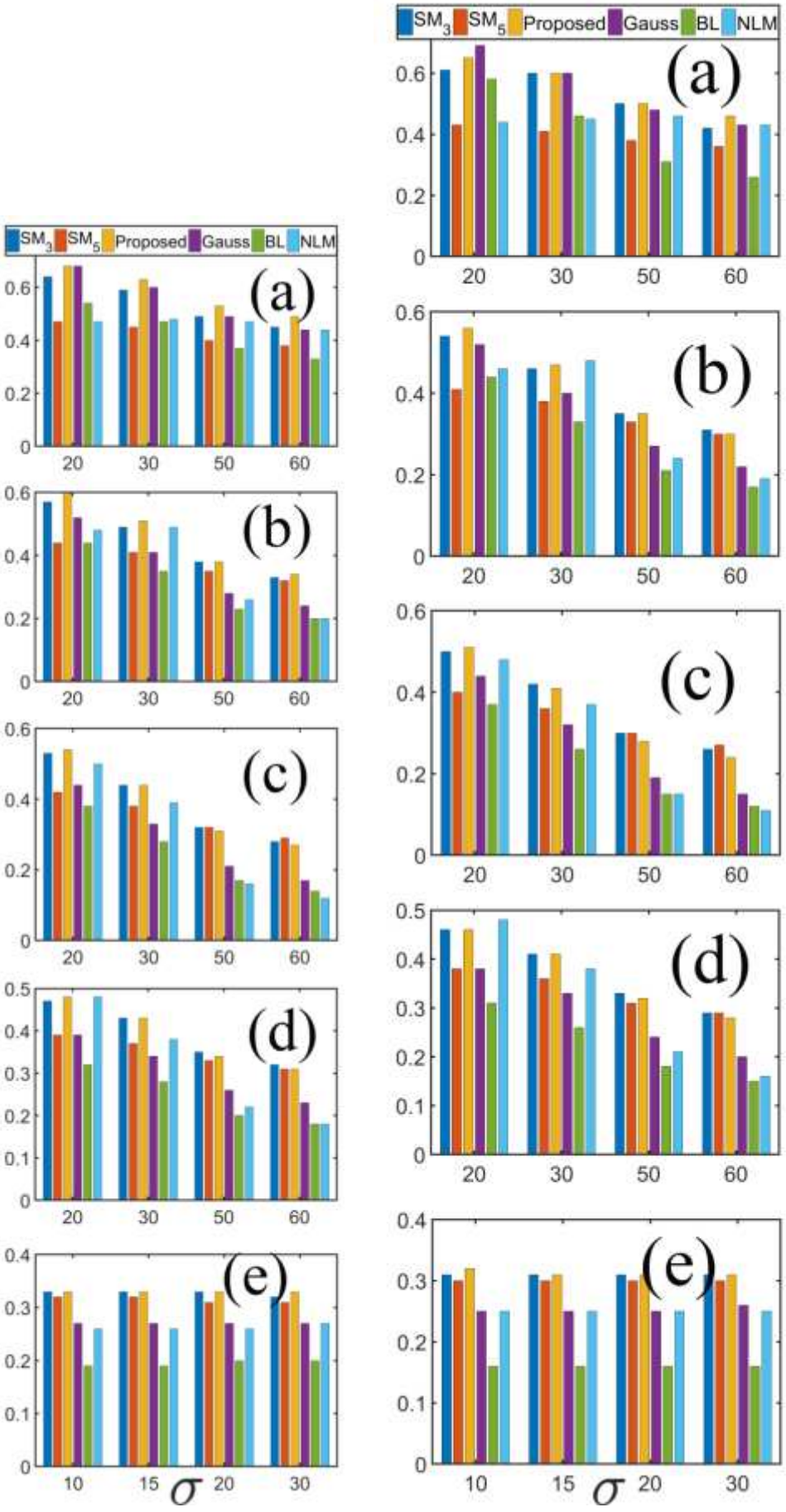
SM3
SM5
Proposed
Gauss
BL
NLM
(a)
(b)
(c)
(d)
(e)
20
30
50
60
10
15
20
30
σ